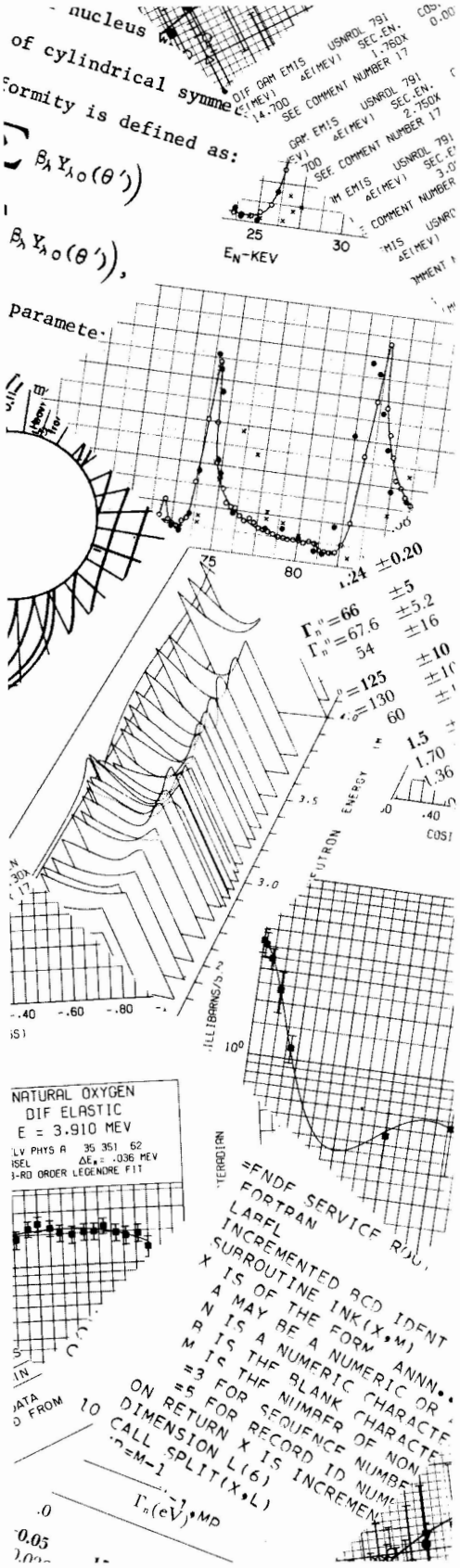

BNL 50388
(ENDF-190)

AN ANALYSIS OF THE ^{239}Pu NEUTRON CROSS SECTIONS FROM 20 keV TO 20 MeV

A. PRINCE, M.K. DRAKE, AND P. HLAVAC

April 1973

NATIONAL NEUTRON CROSS SECTION CENTER
BROOKHAVEN NATIONAL LABORATORY
UPTON, NEW YORK 11973

BNL 50388
(ENDF-190)
(Physics - TID-4500)

AN ANALYSIS OF THE ^{239}Pu NEUTRON CROSS SECTIONS FROM 20 keV TO 20 MeV

by

A. PRINCE, M.K. DRAKE,* AND P. HLAVAC

April 1973

*Present address: Science Applications Inc., La Jolla, California 92037.

NATIONAL NEUTRON CROSS SECTION CENTER
BROOKHAVEN NATIONAL LABORATORY
ASSOCIATED UNIVERSITIES, INC.
UNDER CONTRACT NO. AT(30-1)-16 WITH THE
UNITED STATES ATOMIC ENERGY COMMISSION

NOTICE

Printed in the United States of America
Available from
National Technical Information Service
U.S. Department of Commerce
5285 Port Royal Road
Springfield, Virginia 22151
Price: Printed Copy $3.00; Microfiche $0.95

June 1973 1100 copies

PLUTONIUM NEUTRON-PARTICLE CROSS SECTION

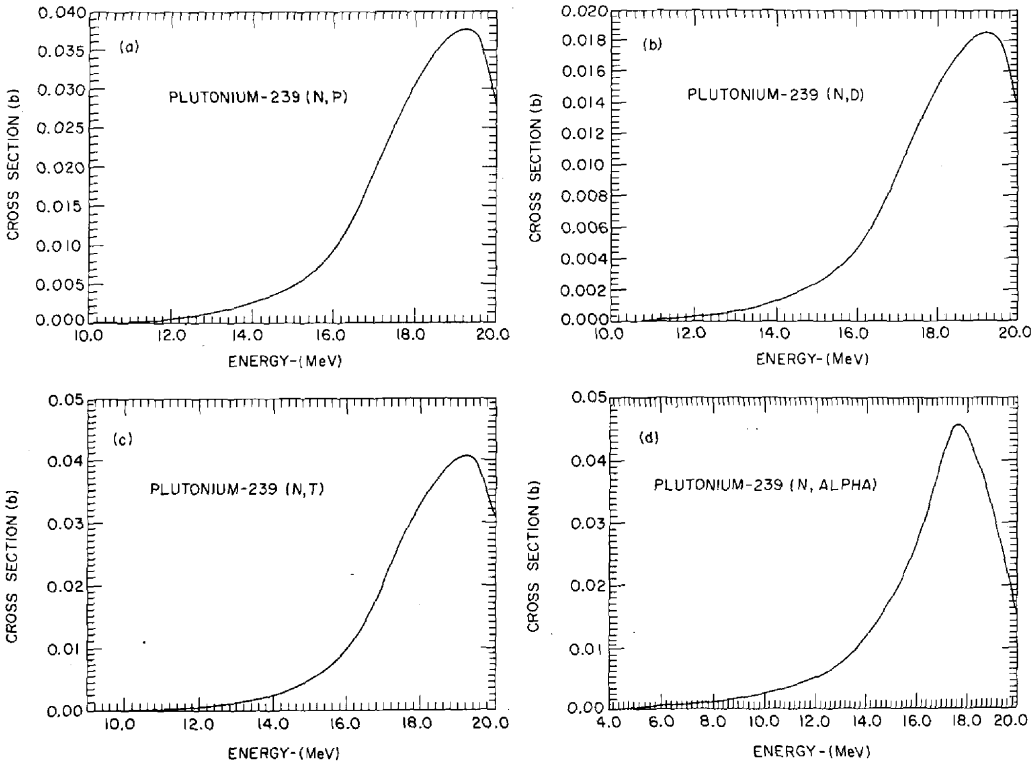

Figure 25

FIGURES

PLUTONIUM-239 INELASTIC CROSS SECTIONS

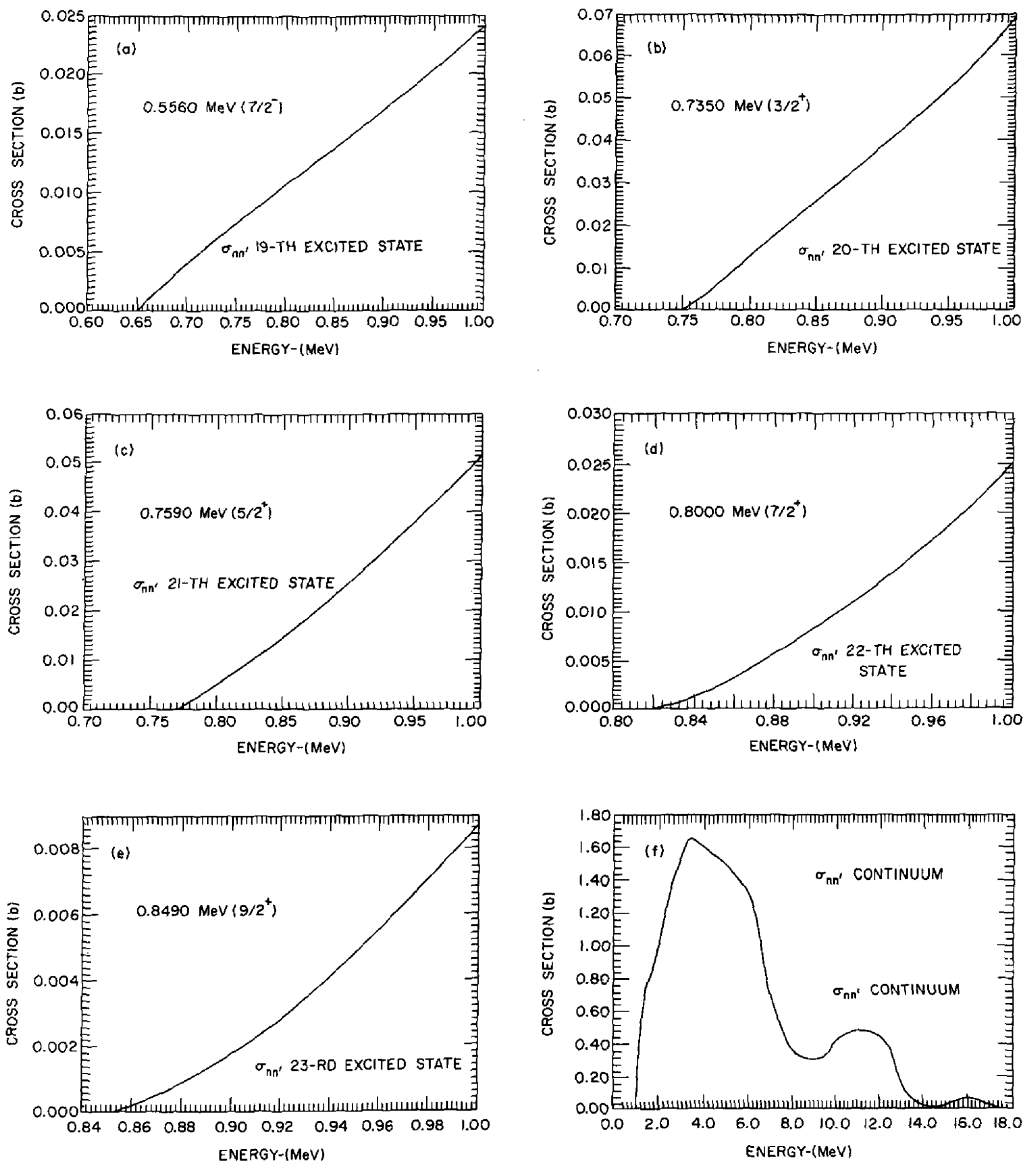

Figure 22

PLUTONIUM-239 INELASTIC CROSS SECTIONS

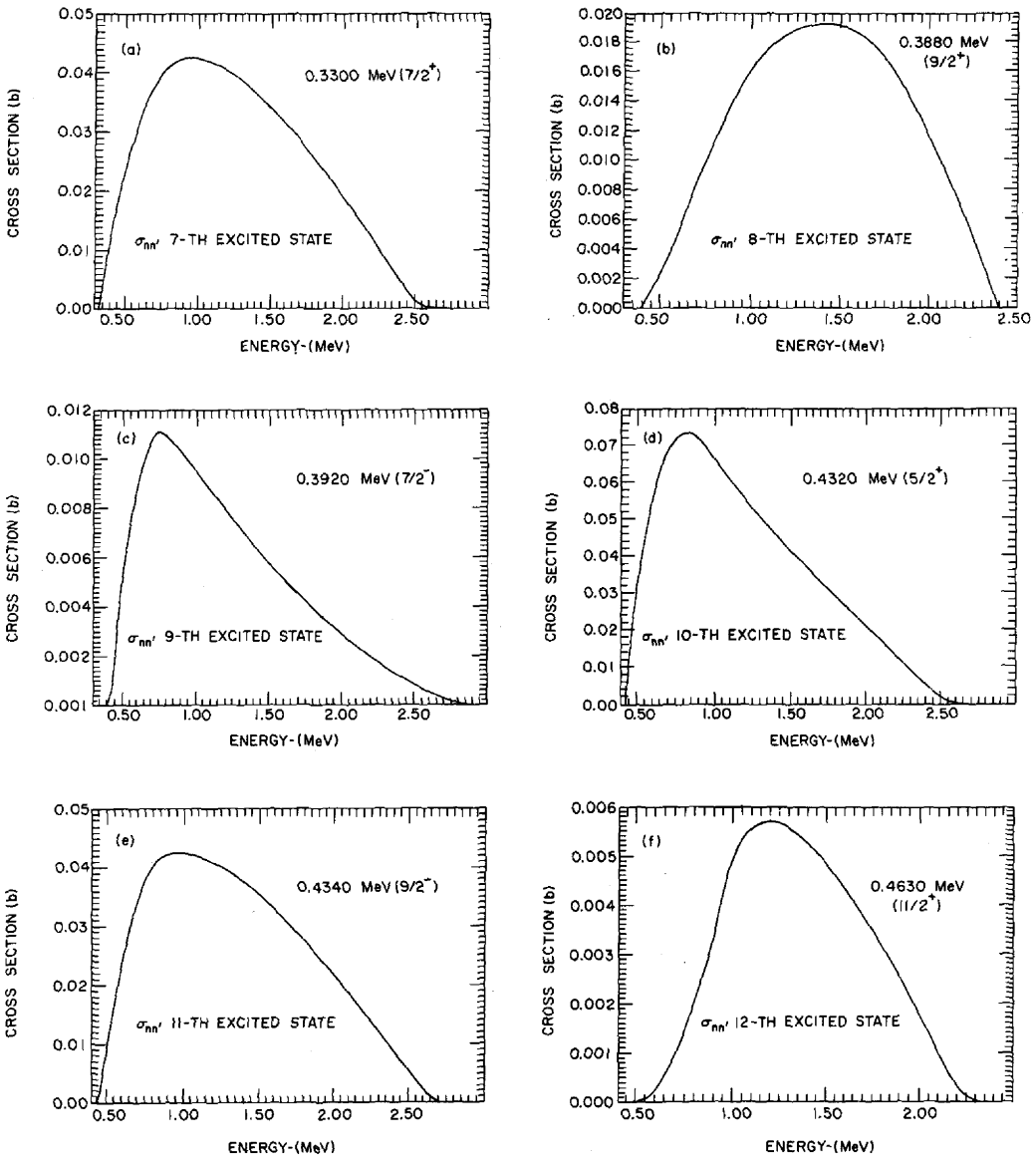

Figure 20

has steadily increased and in most cases exceeds the accuracy of experimental differential data. A clear example of the latter is the proper interpretation of the inelastic scattering cross sections for Pu-239.

An earlier evaluation of $\sigma_{nn'}$ and other reaction cross sections was presented at the Helsinki Conference, June 1970[1] (hereafter referred to as P). This analysis was to form the basis for the high energy (E > 100 keV) cross sections for the Evaluated Nuclear Data File (ENDF/B) on Pu-239. A subsequent meeting of the Cross Section Evaluation Working Group (CSEWG) resulted in expressions of concern that the elastic cross sections in ENDF/B-II were lower than those in ENDF/B-I and the inelastic cross sections were higher.

As pointed out in P, previous calculations used in evaluating Pu-239 have employed a spherical optical potential with the various reaction cross sections being interpreted as arising only from compound nucleus formation. However, since this nuclide is known to exhibit a high degree of deformity, the scattering of neutrons cannot be described adequately by the conventional optical model, which does not consider the coupling between the incident neutron motion and the nuclear surface rotation. This coupling causes the direct excitation of the rotational levels by inelastic scattering.

While these previous analyses have provided fairly good agreement between calculated and experimental angular distributions, the magnitude of the diffraction minima and maxima has not been well produced. Earlier investigations[2,3] have shown that neglecting the high degree of anistropy exhibited by the direct inelastic component can lead to serious errors in the prediction of the differential elastic and inelastic cross sections. These errors manifest themselves in two major areas. In the low

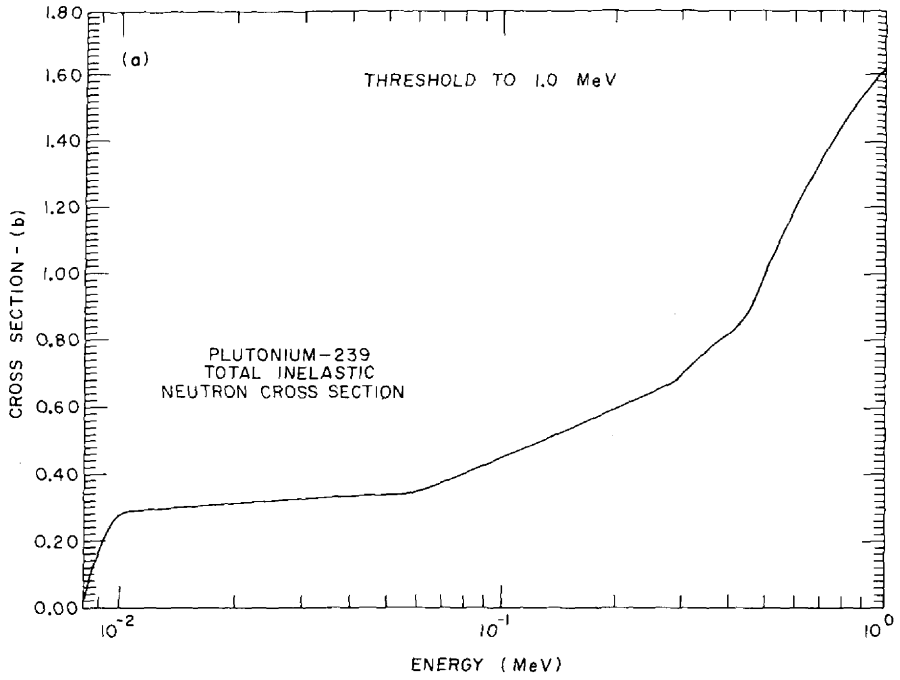

Figure 17

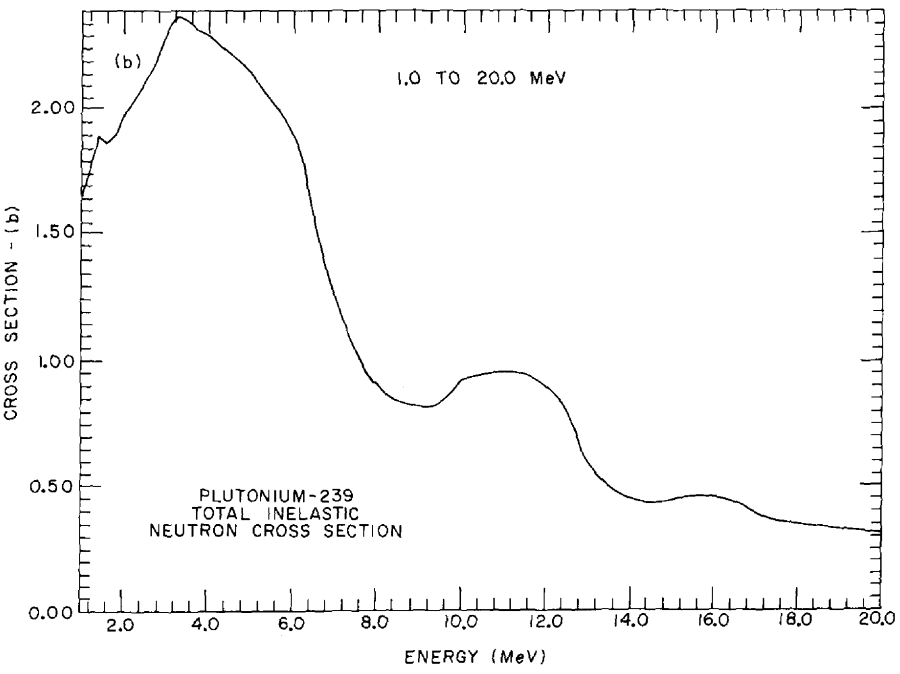

Figure 18

experimental constraints; namely, the total cross section σ_T, the potential scattering cross section σ_{pot}, and the s- and p-wave strength functions (S_0 and S_1).

Two additional pseudo-constraints σ_{nf} and $\sigma_{n\gamma}$ were also introduced in the statistical analysis such that the calculated values agreed to at least 5 to 7% of the most recent recommended values. The reason for the latter restriction is manifested in the fact that such an analysis would beget more confidence in the resulting inelastic processes.

These restrictions were very successful in providing a consistent set of parameters for performing calculations that produced very good agreement with all available experimental data from 10 keV to 20 MeV.

Theory

The differential cross sections for shape elastic scattering (σ_{SE}), the total reaction cross section (σ_R), and the direct inelastic scattering ($\sigma_{(rot)}$) were calculated using the Coupled Channel Code JUPITER I by Tamura[4].

In the phenomenological description it is assumed that the whole interaction to which the neutron is subjected may be described by an optical-model potenital $V(r,\theta,\varphi)$ which is complex and includes spin orbit coupling. Its radial dependence is of the Saxon-Woods form and its derivative. $V(r,\theta,\varphi)$ is assumed to be, in general, non-spherical and is defined as[4]:

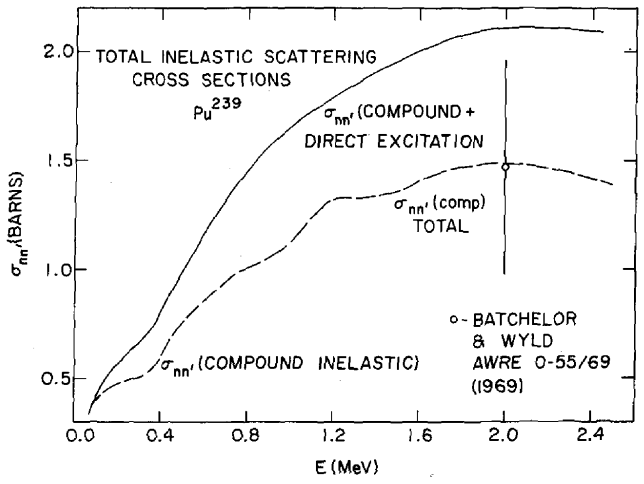

Figure 14

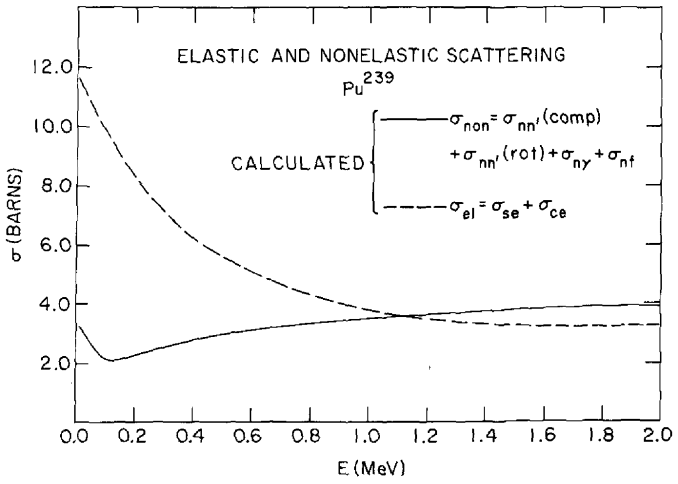

Figure 15

as to incorporate the more recent methods in the analysis of continuum particle emission. The following description is based on the procedures outlined in Ref. (5); for a more complete analysis the reader should consult this work.

From Moldauer[6,7] the reaction cross section for incident channel c and outgoing channel c' ($c \equiv n\ell j$) may be written as:

$$\langle \sigma_{cc'} \rangle = \pi \lambda_c^2 \left[\frac{\langle \theta_{\lambda c} \rangle \langle \theta_{\lambda c'} \rangle}{\langle \theta_\lambda \rangle} W_{cc'} - \frac{\delta_{cc'}}{4} Q_c \langle \theta_{\lambda c} \rangle^2 \right] \tag{1}$$

where

$$\theta_\lambda = \sum_\alpha \langle \theta_{\lambda\alpha} \rangle \qquad \alpha \equiv \text{all open channels.} \tag{2}$$

$$W_{cc'} = \left\langle \frac{\theta_{\lambda c} \theta_{\lambda c'}}{\theta_\lambda} \right\rangle \Bigg/ \frac{\langle \theta_{\lambda c} \rangle \langle \theta_{\lambda c'} \rangle}{\langle \theta_\lambda \rangle} \ . \tag{3}$$

and

$$\langle \theta_{\lambda c} \rangle = T_c + \frac{1}{Q_c} \left[1 - \sqrt{1 - Q_c T_c} \right]^2 \ . \tag{4}$$

T_c is the optical model penetrability for channel c, and Q_c is the statistical parameter with range $0 \leq Q_c \leq 2$.

In previous calculations using ABACUS-NEARREX[9] the quantity Q_c was treated as a constant where its dependence on $\langle \theta_{\lambda c} \rangle$ was ignored. However, as was discovered in several instances during the analysis in P and also reported by[10], such a treatment can lead to negative values for the compound elastic cross section for some partial waves when many channels are open and Q_c is not taken sufficiently small.

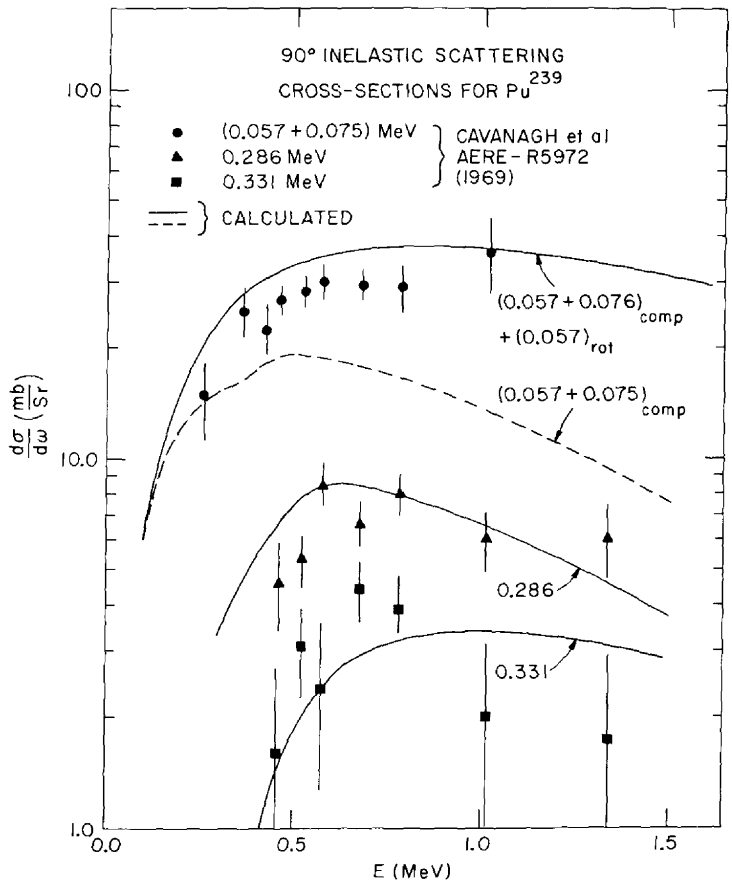
90° INELASTIC SCATTERING
CROSS-SECTIONS FOR Pu239
(0.057 + 0.075) MeV
0.286 MeV
0.331 MeV
CAVANAGH et al
AERE - R5972
(1969)
CALCULATED
(0.057 + 0.076)comp
+ (0.057)rot
(0.057 + 0.075)comp
0.286
0.331
dσ/dω (mb/Sr)
100
10.0
1.0
0.0
0.5
1.0
1.5
E (MeV)

Figure 11

Lane and Lynn[12] and Brown[13].

The fission cross section was interpreted in terms of the Hill-Wheeler[14] model with

$$\langle \theta_{\lambda f} \rangle^{J\pi} = \frac{N^{J\pi}}{2\pi} ,$$

where $N^{J\pi}$ is the effective number of fission channels and is dependent upon the penetrability factor P_i by

$$N^{J\pi} = \sum_i P_i$$

and

$$P_i = \frac{1}{1 + \exp\left[\frac{2\pi(E_{fi}^{J\pi} - E)}{\hbar\omega}\right]} .$$

E_{fi} is the fission threshold, and $\hbar\omega$ the characteristic energy of the barrier curvature.

Combining the coupled-channel calculations with the statistical model produced the following interaction cross sections:

σ_T	= total cross section
σ_{SE}	= shape elastic cross section
σ_{CE}	= compound elastic cross section
σ_{el}	= $\sigma_{SE} + \sigma_{CE}$ total elastic
σ_R	= reaction cross section
σ_C	= compound formation cross section
$\sigma_{nn'}$,(comp.)	= compound inelastic cross section
$\sigma_{nn'}$,(rot.)	= direct inelastic cross section.

Computer code THRESH[15] which is an empirical model embodying the evaporation theory of Weisskopf was used to calculate the $\sigma_{n,2n}$, $\sigma_{n,3n}$, σ_{np}, σ_{nd}, σ_{nt}, and $\sigma_{n\alpha}$ cross sections.

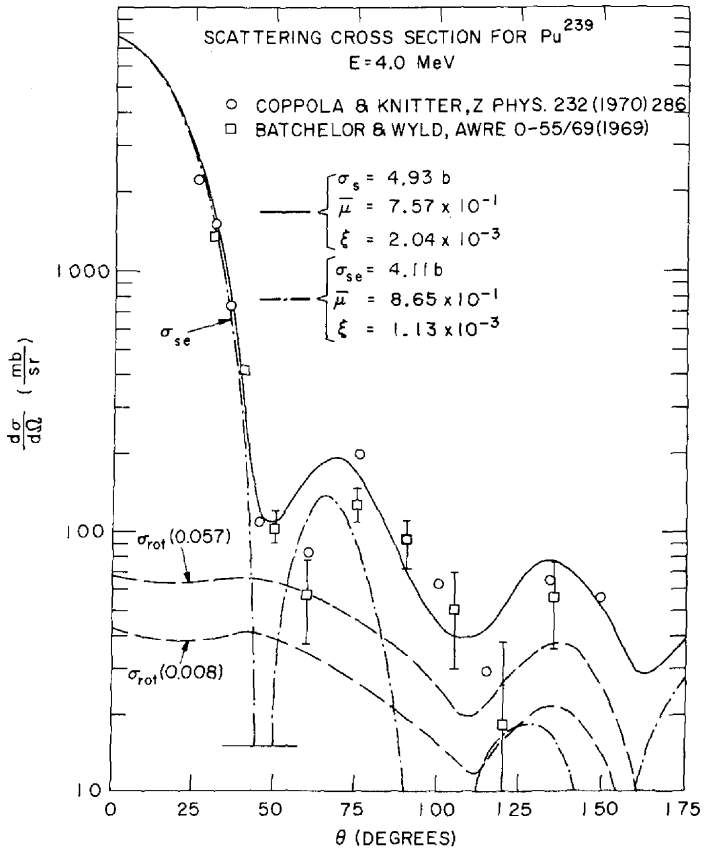
SCATTERING CROSS SECTION FOR Pu239
E=4.0 MeV
COPPOLA & KNITTER, Z PHYS. 232 (1970) 286
BATCHELOR & WYLD, AWRE O-55/69(1969)
σs = 4.93 b
μ̄ = 7.57 x 10-1
ξ = 2.04 x 10-3
σse = 4.11 b
μ̄ = 8.65 x 10-1
ξ = 1.13 x 10-3
σse
σrot (0.057)
σrot (0.008)
dσ/dΩ (mb/sr)
1000
100
10
0
25
50
75
100
125
150
175
θ (DEGREES)

Figure 9

The thresholds for the n,2n, n,3n, and charged particle emission were taken from Ref. (21) and are given below

Reaction	$E_{thresh.}$ (MeV)
n-2n	5.68
n-3n	12.71
n-p	-0.06
n-d	3.96
n-t	3.18
n-He^3	3.68
n-He^4	-11.79

In order to ascertain the quality of the resultant calculation and perhaps to gain a clearer insight into the apparent enigmatic features of the inelastic and elastic scattering processes in Pu-239, it was decided to carry out the calculations which would include the exact energies described in the most recent differential measurements of the microscopic data. These include the following, Knitter and Coppola[22], Cavanagh, et al.[23], Batchelor and Wyld[24], Coppola and Knitter[25], and A. B. Smith[26].

Calculations and Comparison with Experiment

The total cross section for Pu-239 in the energy range 0.001 MeV $\leq$ E $\leq$ 0.1 MeV is shown in Fig. 1 and is compared with the experimental data of Uttley[17]. Along with the calculated values of this work is the evaluation due to Barre, et al.[28] In both cases the agreement with Uttley's experimental points is very good, deviating only slightly around 50 keV.

The s- and p-wave strength functions at 1 keV were calculated to be 1.19×10^{-4} and 1.71×10^{-4}, respectively, which may be compared

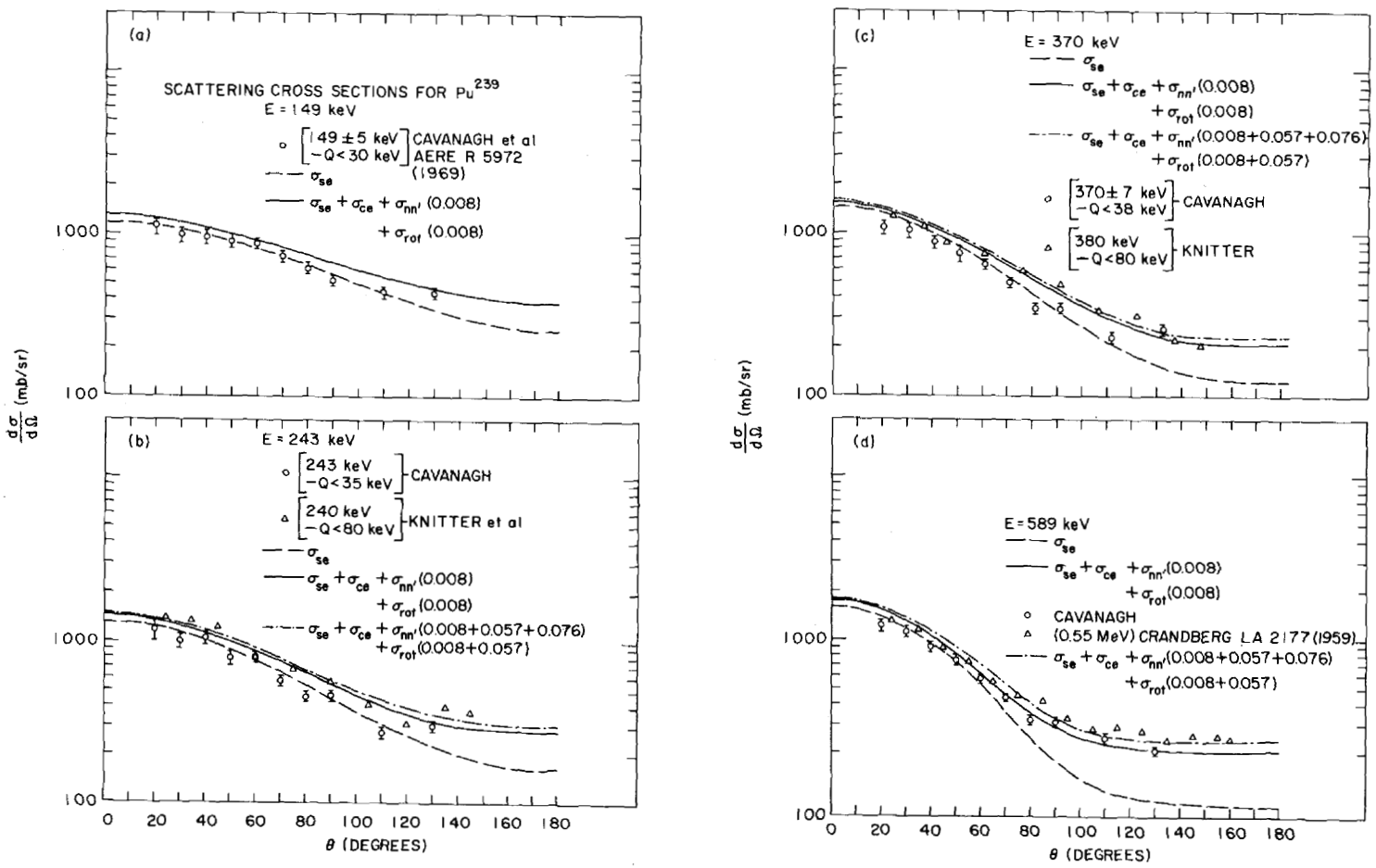
(a)
SCATTERING CROSS SECTIONS FOR Pu239
E = 149 keV
149 ± 5 keV
−Q < 30 keV
CAVANAGH et al
AERE R 5972
(1969)
σse
σse + σce + σnn' (0.008)
+ σrot (0.008)
(b)
E = 243 keV
243 keV
−Q < 35 keV
CAVANAGH
240 keV
−Q < 80 keV
KNITTER et al
σse
σse + σce + σnn' (0.008)
+ σrot (0.008)
σse + σce + σnn' (0.008+0.057+0.076)
+ σrot (0.008+0.057)
(c)
E = 370 keV
σse
σse + σce + σnn' (0.008)
+ σrot (0.008)
σse + σce + σnn' (0.008+0.057+0.076)
+ σrot (0.008+0.057)
370 ± 7 keV
−Q < 38 keV
CAVANAGH
380 keV
−Q < 80 keV
KNITTER
(d)
E = 589 keV
σse
σse + σce + σnn' (0.008)
+ σrot (0.008)
CAVANAGH
(0.55 MeV) CRANDBERG LA 2177 (1959)
σse + σce + σnn' (0.008+0.057+0.076)
+ σrot (0.008+0.057)
dσ/dΩ (mb/sr)
1000
100
0 20 40 60 80 100 120 140 160 180
θ (DEGREES)

Figure 7

the data of Smith (ANL) and Heaton (NBS) (received after the completion of this evaluation).

In Figure 3, the evaluated total cross section is shown to be in excellent agreement with empirical data of Smith (ANL), Heaton et al. (NBS), and Foster and Glasgow,[34] however, the data of Cabe is about 5% higher than the others.

In Figures 4 and 5, the calculated values of the fission cross sections are compared with the experimental data available in the SCISRS data library, and the recommended data of the CSEWG Task Force. It is clearly seen that the calculational results are, in general, within 0.1 to 0.2 barns of the recommended values and well within the accuracy of the experimental data. The wide dispersion in the experimental data points illustrates another region wherein model calculations could possibly aid in unraveling the inconsistencies that exist in the experimental data.

The radiative capture cross section was also calculated for the 0.01 to 1.0 MeV region and up to about 0.5 MeV (discrete inelastic) region, the COMNUC code provided surprisingly good results when compared with the recommended ENDF/B III capture cross section. It should be remembered that the ENDF/B III evaluated cross sections were based on the previously mentioned fission data and recent experimental α values. Thus, any errors in either of these quantities will be manifested in the recommended capture cross section. Above 0.5 MeV, the calculated capture cross section was somewhat larger than the recommended cross

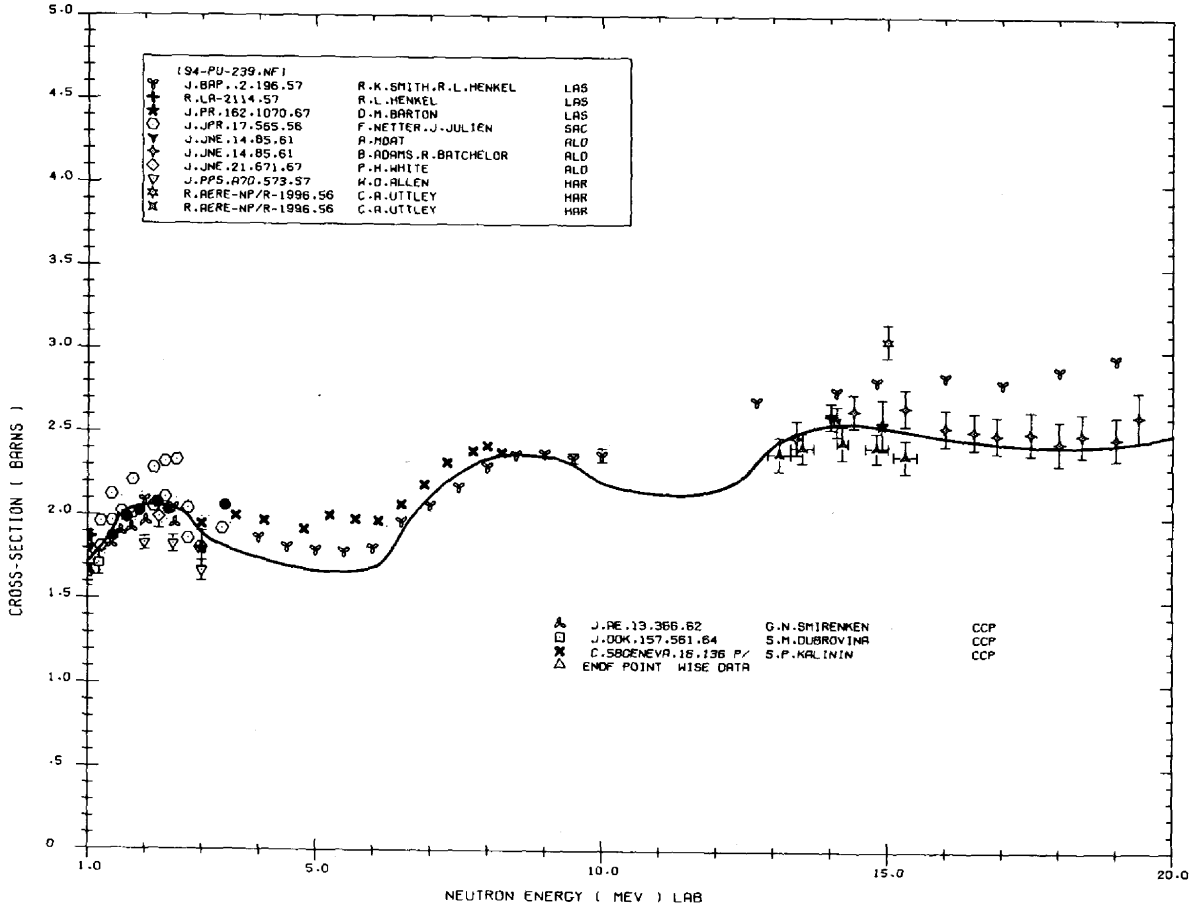
(94-PU-239.NFI
J.BAP.,2.196.57 R.K.SMITH,R.L.HENKEL LAS
R.LA-2114.57 R.L.HENKEL LAS
J.PR.162.1070.67 D.M.BARTON LAS
J.JPR.17.565.56 F.NETTER,J.-J.JULIEN SAC
J.JNE.14.85.61 A.MOAT ALO
J.JNE.14.85.61 B.ADAMS,R.BATCHELOR ALO
J.JNE.21.671.67 P.H.WHITE ALO
J.PPS.A70.573.57 W.O.ALLEN HAR
R.AERE-NP/R-1996.56 C.A.UTTLEY HAR
R.AERE-NP/R-1996.56 C.A.UTTLEY HAR
J.AE.13.366.62 G.N.SMIRENKIN CCP
J.OOK.157.561.64 S.M.DUBROVINA CCP
C.58GENEVA.16.136 P/ S.P.KALININ CCP
ENDF POINT WISE DATA
CROSS-SECTION (BARNS)
NEUTRON ENERGY (MEV) LAB
0
.5
1.0
1.5
2.0
2.5
3.0
3.5
4.0
4.5
5.0
1.0
5.0
10.0
15.0
20.0

Figure 5

A comparison of the differences that become evident when the high degree of anisotropy of these low lying levels is ignored is given in Table IV, where the Legendre coefficients* at 4.0 MeV were calculated from the angular distibutions shown in Figure 9. The average cosine of the scattering angle in the Lab system, μ_L, and the average logarithmic energy decrement per elastic collision, ξ, are given in Figure 9 and at the botton of Table IV. The contribution of the compound elastic and inelastic (first two levels) at 4.0 MeV are of the order 10^{-5} mb/sr and are therefore ignored in Figure 9 and Table IV. Note that including the anisotropic contributions changes the scattering cross section by about 20% while μ_L and ξ are changed by 14% and 45% respectively.

Figure 10 provides a rather vivid description of the interpretation of the experimental scattering data. The dashed curve shown what is referred to as "pure elastic" scattering ($\sigma_{el} = \sigma_{SE} + \sigma_{CE}$). The dash-dot curve includes contributions from direct and compound inelastic excitation of the 8 keV level and should be compared with A. B. Smith's data up to at least 1.1 MeV. To describe the data of Knitter and Coppola[22], one must consider the contributions from the first 3 levels above the ground state. From Figure 10 it is obvious that such evaluatory considerations do produce rather satisfactory agreement with the experimental data.

Figure 11 shows the differential inelastic scattering of Cavanagh, et al.[23] at 90° for a combination of the 57 and 76 keV levels and separate excitations for the 286 and 331 keV levels respectively. It is

*The Legendre coefficients in Table IV are for illustrative purpose only. In ENDF/B III, 20 Legendre coefficients are used to describe the elastic angular distribution, with $\bar{\mu} = 0.8759$ and $\xi = 0.00105$, $\sigma_{SE} = 3.98$ b, $\sigma_{CE} = 0.0$ b.

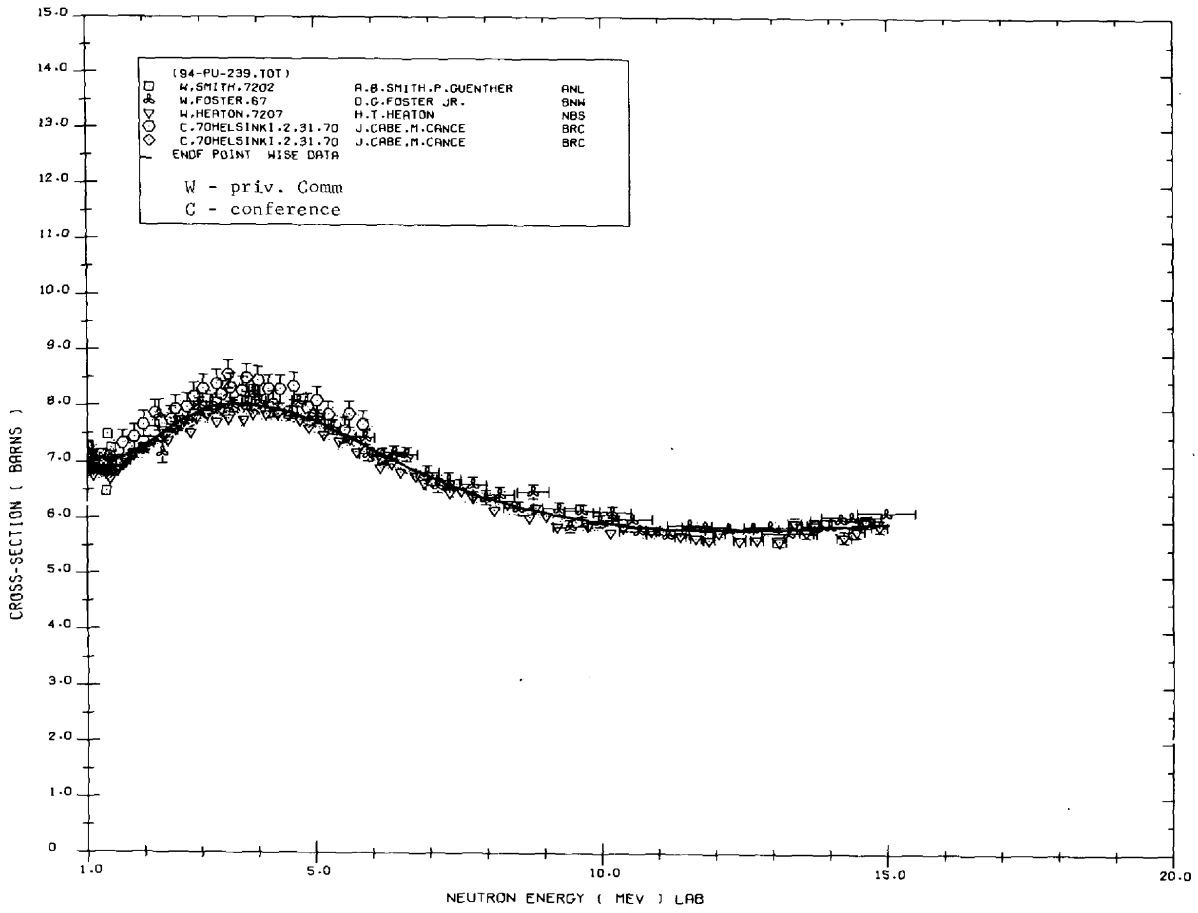
(94-PU-239.TOT)
W,SMITH.7202 A.B.SMITH,P.GUENTHER ANL
W,FOSTER.67 D.G.FOSTER JR. BNW
W,HEATON.7207 H.T.HEATON NBS
C,70HELSINKI.2,31.70 J.CABE,M.CANCE BRC
C,70HELSINKI.2,31.70 J.CABE,M.CANCE BRC
ENDF POINT WISE DATA
W - priv. Comm
C - conference
CROSS-SECTION (BARNS)
NEUTRON ENERGY (MEV) LAB
15.0
14.0
13.0
12.0
11.0
10.0
9.0
8.0
7.0
6.0
5.0
4.0
3.0
2.0
1.0
0
1.0
5.0
10.0
15.0
20.0

Figure 3

Conclusion

Since the accuracy requirements for Pu-239 in analyzing fast reactors has become more demanding, it was necessary to apply the most sophisticated theoretical concepts in the evaluation.

In order to explain the experimental angular distirbution data, the effects of deformation leading to the direct rotational excitation had to be considered.

It was also important that the various compound nucleus reactions, $\sigma_{nn'}$, σ_{nf}, $\sigma_{n\gamma}$, etc. be analyzed in a consistent manner so as to properly define their competitive characteristics.

These factors coupled with comparison with the most recent experimental data have produced what is hoped to be a very important intermediary for a logical evaluation which should prove to be adequate in the analysis of fast reactors which use Pu-239 as fuel.

All calculations used in this evaluation were completed by February 1972.

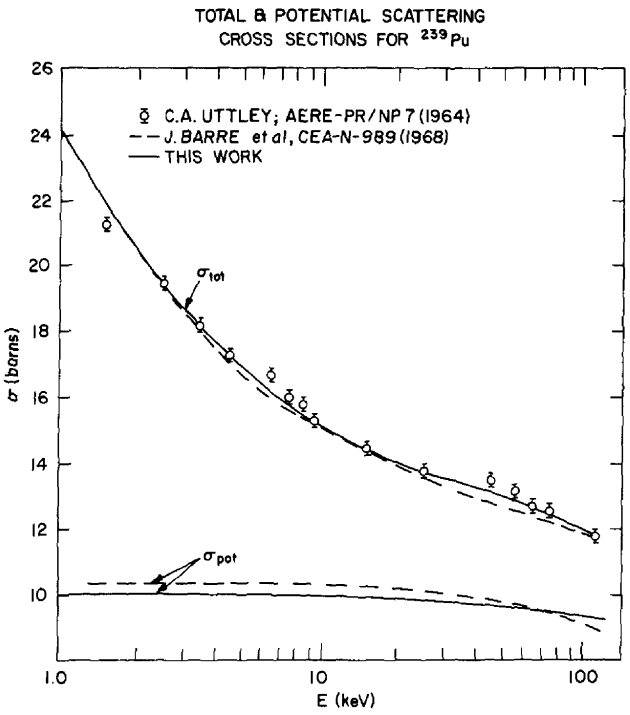
TOTAL & POTENTIAL SCATTERING
CROSS SECTIONS FOR 239Pu
C.A. UTTLEY; AERE-PR/NP 7 (1964)
J. BARRE et al, CEA-N-989 (1968)
THIS WORK
σtot
σpot
σ (barns)
E (keV)
26
24
22
20
18
16
14
12
10
1.0
10
100

Figure 1

(24) R. Batchelor and K. Wyld. AWRE Rpt. No. 0-55/69 (1969).

(25) M. Coppola and H. H. Knitter. Z. Phys. 232 (1970) 286.

(26) A. B. Smith. Argonne Nat'l Lab. (Priv. Comm),

(27) C. A. Uttley. AERE-PR/NP-9 (1965).

(28) J. Y. Barre, et al. CEA-N-989 (1968) EANDC(EUR)-111.

(29) H. Derrien. Int. Conf. Nuclear Data For Reactors (Proc. Conf., Paris 1966) II, IAEA, Vienna (1967) 195.

(30) Yu. V. Ryabov. Sov. J. Nucl. Phys. 5 (1967) 657.

(31) C. A. Uttley. Int. Conf. Study of Nuclear Structure With Neutrons, Vol. I (1965).

(32) L. M. Bollinger, et al. Proc. Geneva Conf. 1958, Vol. 15.

(33) D. J. Hughes, et al. Phys. Rev. Lett. 1 (1958) 461.

(34) D. G. Foster, Jr. and D. W. Glasgow. Phys. Rev. 2C (1971) 576.

(35) L. Cranberg. Los Alamos Rpt. LA-2177 (1959).

(36) P. A. Moldauer. Proc. IAEA Seminar on Phys. of Fast and Intermediate reactors, Vienna, 1961, Vol. I.

TABLE IV: Legendre Coefficients (f_ℓ) for Scattering at 4.0 MeV

	Shape Elastic	Total Scattering
ℓ	f_ℓ	f_ℓ
0	1.00000	1.00000
1	8.64369×10^{-1}	7.55472×10^{-1}
2	7.17507×10^{-1}	6.04563×10^{-1}
3	5.70527×10^{-1}	4.73420×10^{-1}
4	4.43269×10^{-1}	3.62644×10^{-1}
5	3.24059×10^{-1}	2.74031×10^{-1}
6	2.04351×10^{-1}	1.68689×10^{-1}
7	9.88382×10^{-2}	8.21425×10^{-2}
8	3.72463×10^{-2}	3.33180×10^{-2}
9	8.51738×10^{-3}	6.80190×10^{-3}
10	9.75251×10^{-4}	7.82202×10^{-4}
11	-2.27483×10^{-5}	-1.85806×10^{-5}
12	3.29125×10^{-6}	2.10669×10^{-6}
13	3.16028×10^{-6}	1.83861×10^{-6}
14	3.62436×10^{-6}	2.08059×10^{-6}

$\sigma_{SE} = 2\pi\int_{-1}^{1} \frac{d\sigma_{SE}}{d\Omega}\, d\mu = 4.11b$ $\sigma_S = 2\pi\int_{-1}^{1} \frac{d\sigma_S}{d\Omega}\, d\mu = 4.93b$

$\bar{\mu}_L = 0.8647$ $\bar{\mu}_L = 0.7567$

$\xi = 0.001128$ $\xi = 0.002037$

TABLE II

Energy Level Scheme

Pu-239		
Level	I^{π}	Excitation (MeV)
0	$1/2^{+}$	0.0000
1	$3/2^{+}$	0.0080
2	$5/2^{+}$	0.0570
3	$7/2^{+}$	0.0760
4	$9/2^{+}$	0.1640
5	$11/2^{+}$	0.1930
6	$5/2^{+}$	0.2860
7	$7/2^{+}$	0.3300
8	$9/2^{+}$	0.3880
9	$7/2^{-}$	0.3920
10	$5/2^{+}$	0.4320
11	$9/2^{-}$	0.4340
12	$11/2^{+}$	0.4630
13	$1/2^{-}$	0.4700
14	$7/2^{+}$	0.4800
15	$11/2^{-}$	0.4860
16	$3/2^{-}$	0.4920
17	$5/2^{-}$	0.5050
18	$7/2^{+}$	0.5120
19	$7/2^{-}$	0.5560
20	$3/2^{+}$	0.7350
21	$5/2^{+}$	0.7590
22	$7/2^{+}$	0.8000
23	$9/2^{+}$	0.8490

TABLE II

Energy Level Scheme

Pu-239		
Level	I^{π}	Excitation (MeV)
0	$1/2^{+}$	0.0000
1	$3/2^{+}$	0.0080
2	$5/2^{+}$	0.0570
3	$7/2^{+}$	0.0760
4	$9/2^{+}$	0.1640
5	$11/2^{+}$	0.1930
6	$5/2^{+}$	0.2860
7	$7/2^{+}$	0.3300
8	$9/2^{+}$	0.3880
9	$7/2^{-}$	0.3920
10	$5/2^{+}$	0.4320
11	$9/2^{-}$	0.4340
12	$11/2^{+}$	0.4630
13	$1/2^{-}$	0.4700
14	$7/2^{+}$	0.4800
15	$11/2^{-}$	0.4860
16	$3/2^{-}$	0.4920
17	$5/2^{-}$	0.5050
18	$7/2^{+}$	0.5120
19	$7/2^{-}$	0.5560
20	$3/2^{+}$	0.7350
21	$5/2^{+}$	0.7590
22	$7/2^{+}$	0.8000
23	$9/2^{+}$	0.8490

TABLE IV: Legendre Coefficients (f_ℓ) for Scattering at 4.0 MeV

	Shape Elastic	Total Scattering
ℓ	f_ℓ	f_ℓ
0	1.00000	1.00000
1	8.64369×10^{-1}	7.55472×10^{-1}
2	7.17507×10^{-1}	6.04563×10^{-1}
3	5.70527×10^{-1}	4.73420×10^{-1}
4	4.43269×10^{-1}	3.62644×10^{-1}
5	3.24059×10^{-1}	2.74031×10^{-1}
6	2.04351×10^{-1}	1.68689×10^{-1}
7	9.88382×10^{-2}	8.21425×10^{-2}
8	3.72463×10^{-2}	3.33180×10^{-2}
9	8.51738×10^{-3}	6.80190×10^{-3}
10	9.75251×10^{-4}	7.82202×10^{-4}
11	-2.27483×10^{-5}	-1.85806×10^{-5}
12	3.29125×10^{-6}	2.10669×10^{-6}
13	3.16028×10^{-6}	1.83861×10^{-6}
14	3.62436×10^{-6}	2.08059×10^{-6}

$\sigma_{SE} = 2\pi\int_{-1}^{1} \frac{d\sigma_{SE}}{d\Omega}\, d\mu = 4.11b$ $\sigma_S = 2\pi\int_{-1}^{1} \frac{d\sigma_S}{d\Omega}\, d\mu = 4.93b$

$\bar{\mu}_L = 0.8647$ $\bar{\mu}_L = 0.7567$

$\xi = 0.001128$ $\xi = 0.002037$

(24) R. Batchelor and K. Wyld. AWRE Rpt. No. 0-55/69 (1969).

(25) M. Coppola and H. H. Knitter. Z. Phys. 232 (1970) 286.

(26) A. B. Smith. Argonne Nat'l Lab. (Priv. Comm),

(27) C. A. Uttley. AERE-PR/NP-9 (1965).

(28) J. Y. Barre, et al. CEA-N-989 (1968) EANDC(EUR)-111.

(29) H. Derrien. Int. Conf. Nuclear Data For Reactors (Proc. Conf., Paris 1966) II, IAEA, Vienna (1967) 195.

(30) Yu. V. Ryabov. Sov. J. Nucl. Phys. 5 (1967) 657.

(31) C. A. Uttley. Int. Conf. Study of Nuclear Structure With Neutrons, Vol. I (1965).

(32) L. M. Bollinger, et al. Proc. Geneva Conf. 1958, Vol. 15.

(33) D. J. Hughes, et al. Phys. Rev. Lett. 1 (1958) 461.

(34) D. G. Foster, Jr. and D. W. Glasgow. Phys. Rev. 2C (1971) 576.

(35) L. Cranberg. Los Alamos Rpt. LA-2177 (1959).

(36) P. A. Moldauer. Proc. IAEA Seminar on Phys. of Fast and Intermediate reactors, Vienna, 1961, Vol. I.

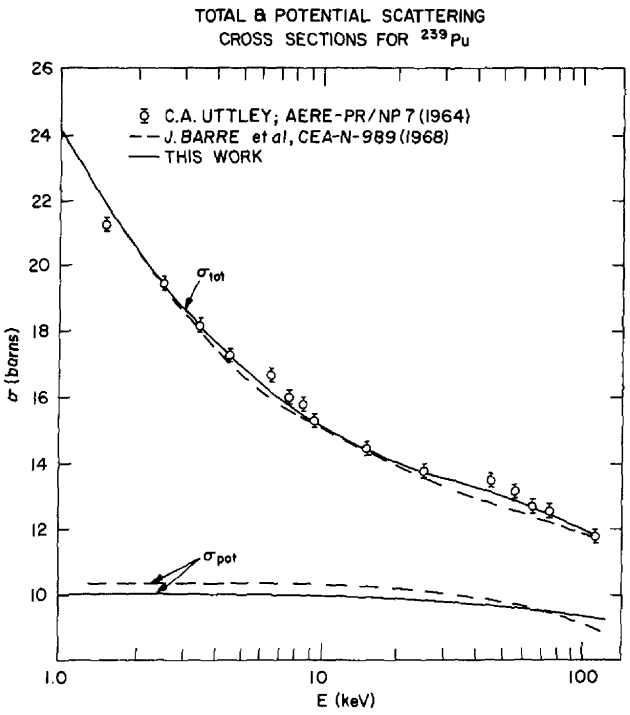
TOTAL & POTENTIAL SCATTERING
CROSS SECTIONS FOR 239Pu
C.A. UTTLEY; AERE-PR/NP 7 (1964)
J. BARRE et al, CEA-N-989 (1968)
THIS WORK
σtot
σpot
σ (barns)
E (keV)
26
24
22
20
18
16
14
12
10
1.0
10
100

Figure 1

Conclusion

Since the accuracy requirements for Pu-239 in analyzing fast reactors has become more demanding, it was necessary to apply the most sophisticated theoretical concepts in the evaluation.

In order to explain the experimental angular distirbution data, the effects of deformation leading to the direct rotational excitation had to be considered.

It was also important that the various compound nucleus reactions, $\sigma_{nn'}$, σ_{nf}, $\sigma_{n\gamma}$, etc. be analyzed in a consistent manner so as to properly define their competitive characteristics.

These factors coupled with comparison with the most recent experimental data have produced what is hoped to be a very important intermediary for a logical evaluation which should prove to be adequate in the analysis of fast reactors which use Pu-239 as fuel.

All calculations used in this evaluation were completed by February 1972.

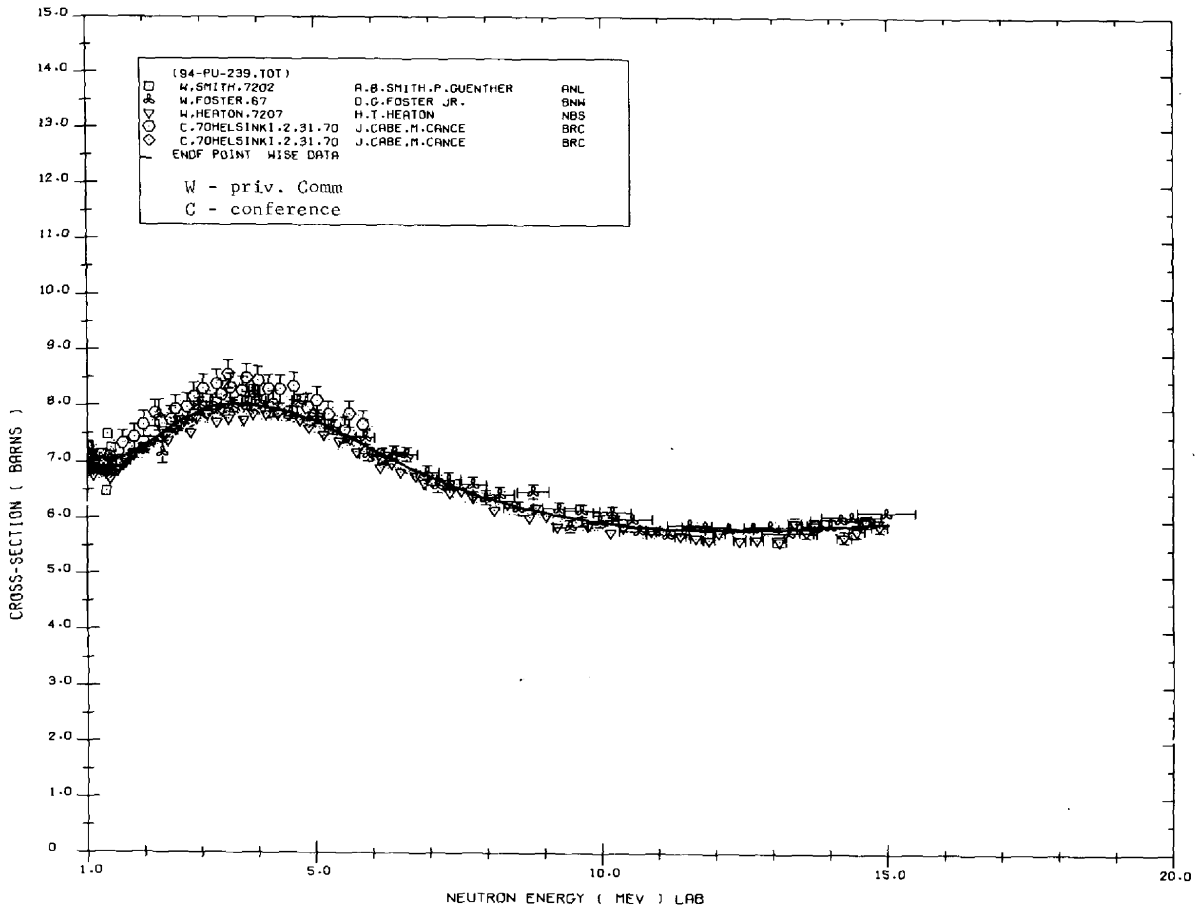
(94-PU-239.TOT)
W,SMITH.7202 A.B.SMITH,P.GUENTHER ANL
W,FOSTER.67 D.G.FOSTER JR. BNW
W,HEATON.7207 H.T.HEATON NBS
C,70HELSINKI.2,31.70 J.CABE,M.CANCE BRC
C,70HELSINKI.2,31.70 J.CABE,M.CANCE BRC
ENDF POINT WISE DATA
W - priv. Comm
C - conference
CROSS-SECTION (BARNS)
NEUTRON ENERGY (MEV) LAB
15.0
14.0
13.0
12.0
11.0
10.0
9.0
8.0
7.0
6.0
5.0
4.0
3.0
2.0
1.0
0
1.0
5.0
10.0
15.0
20.0

Figure 3

A comparison of the differences that become evident when the high degree of anisotropy of these low lying levels is ignored is given in Table IV, where the Legendre coefficients* at 4.0 MeV were calculated from the angular distibutions shown in Figure 9. The average cosine of the scattering angle in the Lab system, μ_L, and the average logarithmic energy decrement per elastic collision, ξ, are given in Figure 9 and at the botton of Table IV. The contribution of the compound elastic and inelastic (first two levels) at 4.0 MeV are of the order 10^{-5} mb/sr and are therefore ignored in Figure 9 and Table IV. Note that including the anisotropic contributions changes the scattering cross section by about 20% while μ_L and ξ are changed by 14% and 45% respectively.

Figure 10 provides a rather vivid description of the interpretation of the experimental scattering data. The dashed curve shown what is referred to as "pure elastic" scattering ($\sigma_{el} = \sigma_{SE} + \sigma_{CE}$). The dash-dot curve includes contributions from direct and compound inelastic excitation of the 8 keV level and should be compared with A. B. Smith's data up to at least 1.1 MeV. To describe the data of Knitter and Coppola[22], one must consider the contributions from the first 3 levels above the ground state. From Figure 10 it is obvious that such evaluatory considerations do produce rather satisfactory agreement with the experimental data.

Figure 11 shows the differential inelastic scattering of Cavanagh, et al.[23] at 90° for a combination of the 57 and 76 keV levels and separate excitations for the 286 and 331 keV levels respectively. It is

*The Legendre coefficients in Table IV are for illustrative purpose only. In ENDF/B III, 20 Legendre coefficients are used to describe the elastic angular distribution, with $\bar{\mu} = 0.8759$ and $\xi = 0.00105$, $\sigma_{SE} = 3.98$ b, $\sigma_{CE} = 0.0$ b.

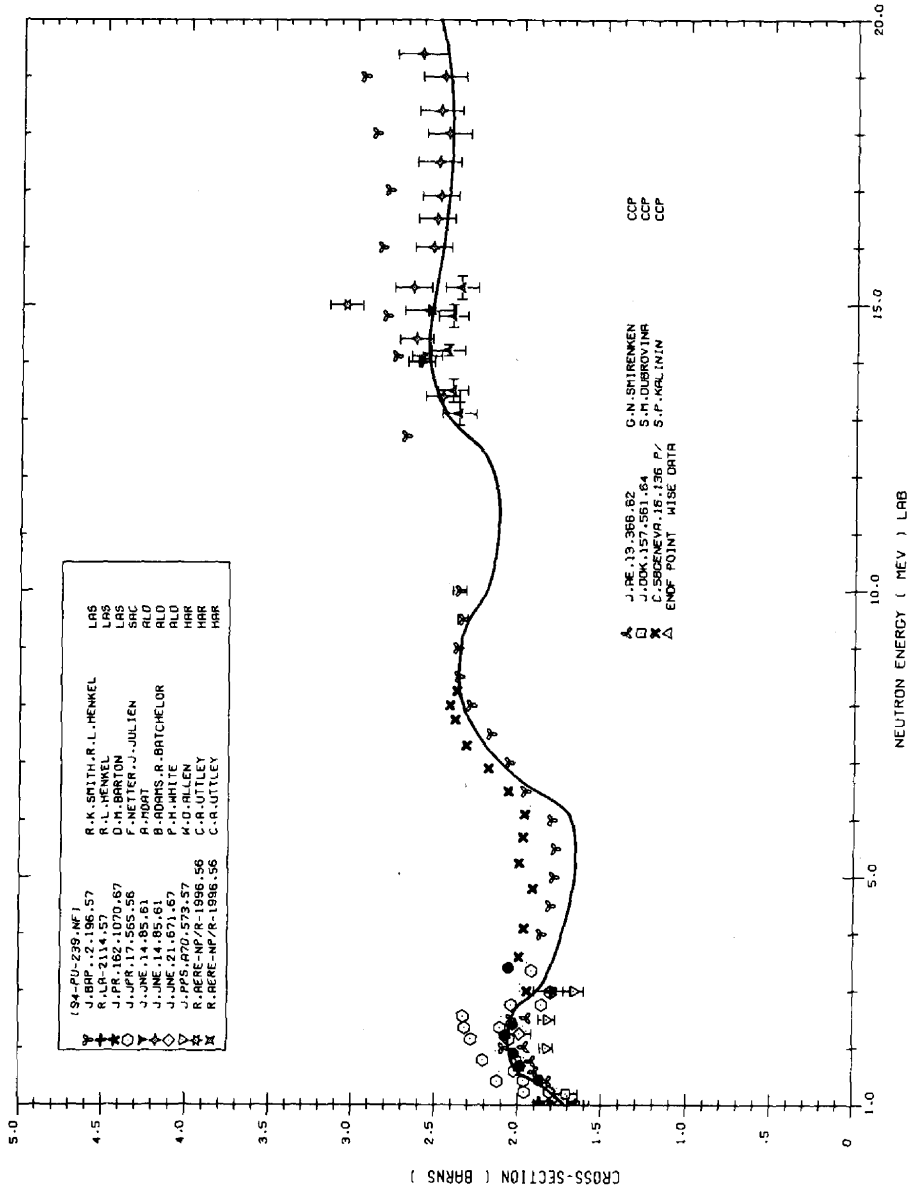
(94-PU-239.NFI
J.BAP.72.196.57 R.K.SMITH.R.L.HENKEL LAS
R.LA-2114.57 R.L.HENKEL LAS
J.PR.162.1070.67 D.M.BARTON LAS
J.JPR.17.565.56 F.NETTER.J.JULIEN SAC
J.JNE.14.85.61 A.MOAT ALO
J.JNE.14.85.61 B.ADAMS.R.BATCHELOR ALO
J.JNE.21.671.67 P.H.WHITE ALO
J.PPS.A70.573.57 W.O.ALLEN HAR
R.AERE-NP/R-1986.56 C.A.UTTLEY HAR
R.AERE-NP/R-1986.56 C.A.UTTLEY HAR
J.NE.13.366.62 G.N.SMIRENKEN CCP
J.DOK.157.561.64 S.M.DUBROVINA CCP
C.58GENEVA.16.136 P/ S.P.KALININ CCP
ENDF POINT WISE DATA
CROSS-SECTION (BARNS)
NEUTRON ENERGY (MEV) LAB
5.0
4.5
4.0
3.5
3.0
2.5
2.0
1.5
1.0
.5
0
1.0
5.0
10.0
15.0
20.0

Figure 5

the data of Smith (ANL) and Heaton (NBS) (received after the completion of this evaluation).

In Figure 3, the evaluated total cross section is shown to be in excellent agreement with empirical data of Smith (ANL), Heaton et al. (NBS), and Foster and Glasgow,[34] however, the data of Cabe is about 5% higher than the others.

In Figures 4 and 5, the calculated values of the fission cross sections are compared with the experimental data available in the SCISRS data library, and the recommended data of the CSEWG Task Force. It is clearly seen that the calculational results are, in general, within 0.1 to 0.2 barns of the recommended values and well within the accuracy of the experimental data. The wide dispersion in the experimental data points illustrates another region wherein model calculations could possibly aid in unraveling the inconsistencies that exist in the experimental data.

The radiative capture cross section was also calculated for the 0.01 to 1.0 MeV region and up to about 0.5 MeV (discrete inelastic) region, the COMNUC code provided surprisingly good results when compared with the recommended ENDF/B III capture cross section. It should be remembered that the ENDF/B III evaluated cross sections were based on the previously mentioned fission data and recent experimental α values. Thus, any errors in either of these quantities will be manifested in the recommended capture cross section. Above 0.5 MeV, the calculated capture cross section was somewhat larger than the recommended cross

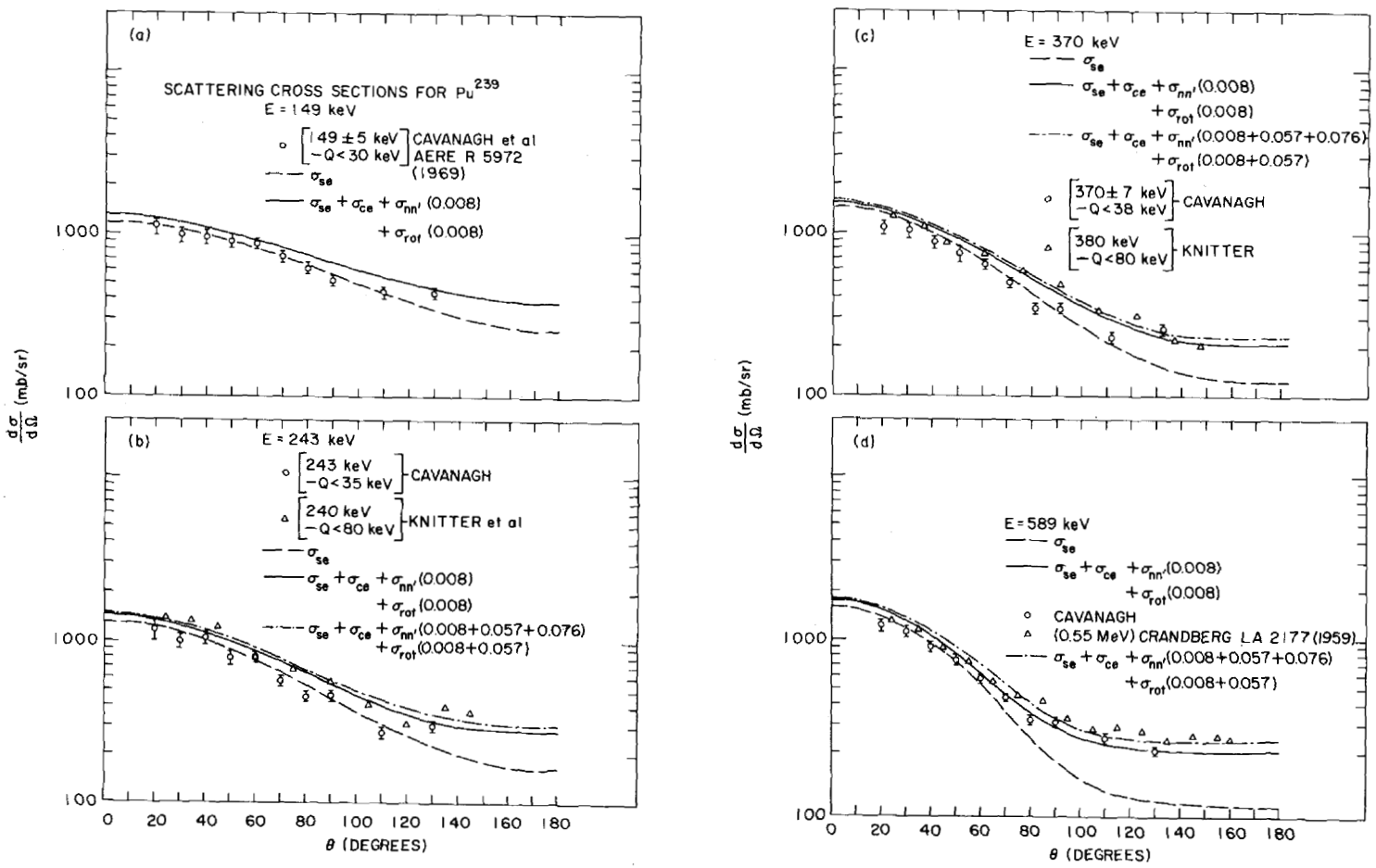
(a)
SCATTERING CROSS SECTIONS FOR Pu239
E = 149 keV
149 ± 5 keV
−Q < 30 keV
CAVANAGH et al
AERE R 5972
(1969)
σse
σse + σce + σnn' (0.008)
+ σrot (0.008)
(b)
E = 243 keV
243 keV
−Q < 35 keV
CAVANAGH
240 keV
−Q < 80 keV
KNITTER et al
σse
σse + σce + σnn' (0.008)
+ σrot (0.008)
σse + σce + σnn' (0.008+0.057+0.076)
+ σrot (0.008+0.057)
(c)
E = 370 keV
σse
σse + σce + σnn' (0.008)
+ σrot (0.008)
σse + σce + σnn' (0.008+0.057+0.076)
+ σrot (0.008+0.057)
370 ± 7 keV
−Q < 38 keV
CAVANAGH
380 keV
−Q < 80 keV
KNITTER
(d)
E = 589 keV
σse
σse + σce + σnn' (0.008)
+ σrot (0.008)
CAVANAGH
(0.55 MeV) CRANDBERG LA 2177 (1959)
σse + σce + σnn' (0.008+0.057+0.076)
+ σrot (0.008+0.057)
dσ/dΩ (mb/sr)
1000
100
0 20 40 60 80 100 120 140 160 180
θ (DEGREES)

Figure 7

The thresholds for the n,2n, n,3n, and charged particle emission were taken from Ref. (21) and are given below

Reaction	$E_{thresh.}$ (MeV)
n-2n	5.68
n-3n	12.71
n-p	-0.06
n-d	3.96
n-t	3.18
n-He^3	3.68
n-He^4	-11.79

In order to ascertain the quality of the resultant calculation and perhaps to gain a clearer insight into the apparent enigmatic features of the inelastic and elastic scattering processes in Pu-239, it was decided to carry out the calculations which would include the exact energies described in the most recent differential measurements of the microscopic data. These include the following, Knitter and Coppola[22], Cavanagh, et al.[23], Batchelor and Wyld[24], Coppola and Knitter[25], and A. B. Smith[26].

Calculations and Comparison with Experiment

The total cross section for Pu-239 in the energy range 0.001 MeV $\leq$ E $\leq$ 0.1 MeV is shown in Fig. 1 and is compared with the experimental data of Uttley[17]. Along with the calculated values of this work is the evaluation due to Barre, et al.[28] In both cases the agreement with Uttley's experimental points is very good, deviating only slightly around 50 keV.

The s- and p-wave strength functions at 1 keV were calculated to be 1.19×10^{-4} and 1.71×10^{-4}, respectively, which may be compared

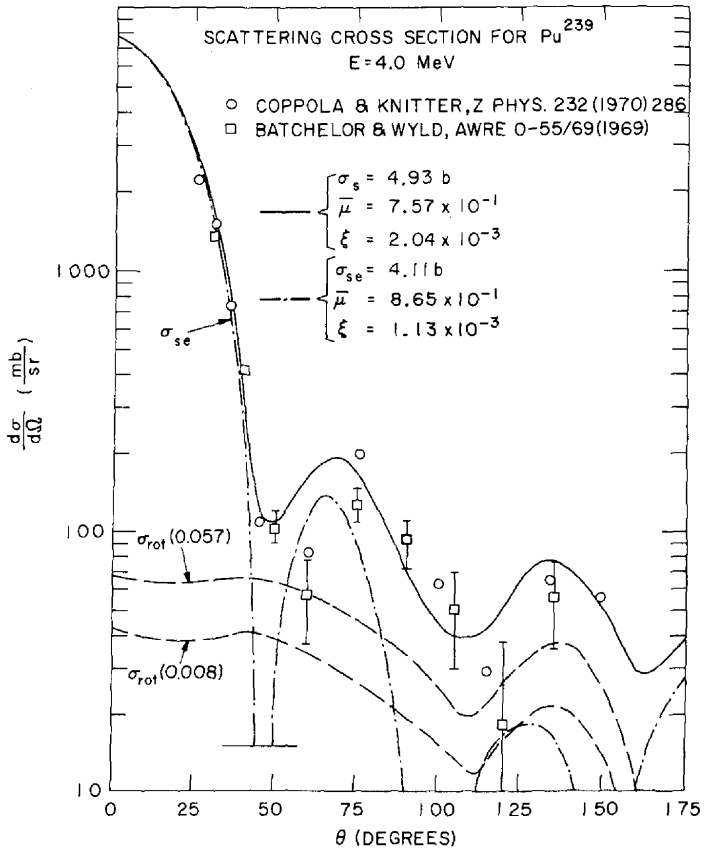
SCATTERING CROSS SECTION FOR Pu239
E=4.0 MeV
COPPOLA & KNITTER, Z PHYS. 232 (1970) 286
BATCHELOR & WYLD, AWRE O-55/69(1969)
σs = 4.93 b
μ̄ = 7.57 x 10-1
ξ = 2.04 x 10-3
σse = 4.11 b
μ̄ = 8.65 x 10-1
ξ = 1.13 x 10-3
σse
σrot (0.057)
σrot (0.008)
dσ/dΩ (mb/sr)
1000
100
10
0
25
50
75
100
125
150
175
θ (DEGREES)

Figure 9

Lane and Lynn[12] and Brown[13].

The fission cross section was interpreted in terms of the Hill-Wheeler[14] model with

$$\langle \theta_{\lambda f} \rangle^{J\pi} = \frac{N^{J\pi}}{2\pi} ,$$

where $N^{J\pi}$ is the effective number of fission channels and is dependent upon the penetrability factor P_i by

$$N^{J\pi} = \sum_i P_i$$

and

$$P_i = \frac{1}{1 + \exp\left[\frac{2\pi(E_{fi}^{J\pi} - E)}{\hbar\omega}\right]} .$$

E_{fi} is the fission threshold, and $\hbar\omega$ the characteristic energy of the barrier curvature.

Combining the coupled-channel calculations with the statistical model produced the following interaction cross sections:

σ_T	= total cross section
σ_{SE}	= shape elastic cross section
σ_{CE}	= compound elastic cross section
σ_{el}	= $\sigma_{SE} + \sigma_{CE}$ total elastic
σ_R	= reaction cross section
σ_C	= compound formation cross section
$\sigma_{nn'}$,(comp.)	= compound inelastic cross section
$\sigma_{nn'}$,(rot.)	= direct inelastic cross section.

Computer code THRESH[15] which is an empirical model embodying the evaporation theory of Weisskopf was used to calculate the $\sigma_{n,2n}$, $\sigma_{n,3n}$, σ_{np}, σ_{nd}, σ_{nt}, and $\sigma_{n\alpha}$ cross sections.

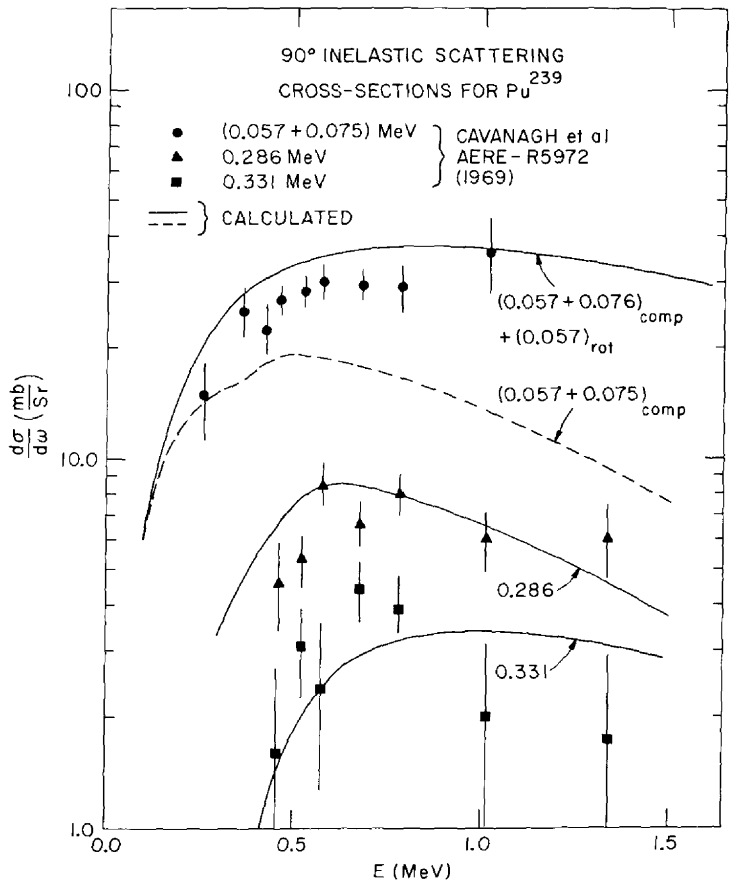
90° INELASTIC SCATTERING
CROSS-SECTIONS FOR Pu239
(0.057 + 0.075) MeV
0.286 MeV
0.331 MeV
CAVANAGH et al
AERE - R5972
(1969)
CALCULATED
(0.057 + 0.076)comp
+ (0.057)rot
(0.057 + 0.075)comp
0.286
0.331
dσ/dω (mb/Sr)
100
10.0
1.0
0.0
0.5
1.0
1.5
E (MeV)

Figure 11

as to incorporate the more recent methods in the analysis of continuum particle emission. The following description is based on the procedures outlined in Ref. (5); for a more complete analysis the reader should consult this work.

From Moldauer[6,7] the reaction cross section for incident channel c and outgoing channel c' ($c \equiv n\ell j$) may be written as:

$$\langle \sigma_{cc'} \rangle = \pi \lambda_c^2 \left[\frac{\langle \theta_{\lambda c} \rangle \langle \theta_{\lambda c'} \rangle}{\langle \theta_\lambda \rangle} W_{cc'} - \frac{\delta_{cc'}}{4} Q_c \langle \theta_{\lambda c} \rangle^2 \right] \tag{1}$$

where

$$\theta_\lambda = \sum_\alpha \langle \theta_{\lambda\alpha} \rangle \qquad \alpha \equiv \text{all open channels.} \tag{2}$$

$$W_{cc'} = \left\langle \frac{\theta_{\lambda c} \theta_{\lambda c'}}{\theta_\lambda} \right\rangle \Bigg/ \frac{\langle \theta_{\lambda c} \rangle \langle \theta_{\lambda c'} \rangle}{\langle \theta_\lambda \rangle} \ . \tag{3}$$

and

$$\langle \theta_{\lambda c} \rangle = T_c + \frac{1}{Q_c} \left[1 - \sqrt{1 - Q_c T_c} \right]^2 \ . \tag{4}$$

T_c is the optical model penetrability for channel c, and Q_c is the statistical parameter with range $0 \leq Q_c \leq 2$.

In previous calculations using ABACUS-NEARREX[9] the quantity Q_c was treated as a constant where its dependence on $\langle \theta_{\lambda c} \rangle$ was ignored. However, as was discovered in several instances during the analysis in P and also reported by[10], such a treatment can lead to negative values for the compound elastic cross section for some partial waves when many channels are open and Q_c is not taken sufficiently small.

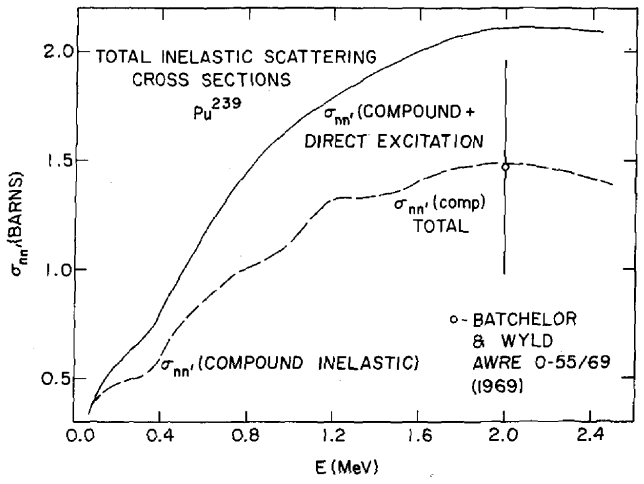

Figure 14

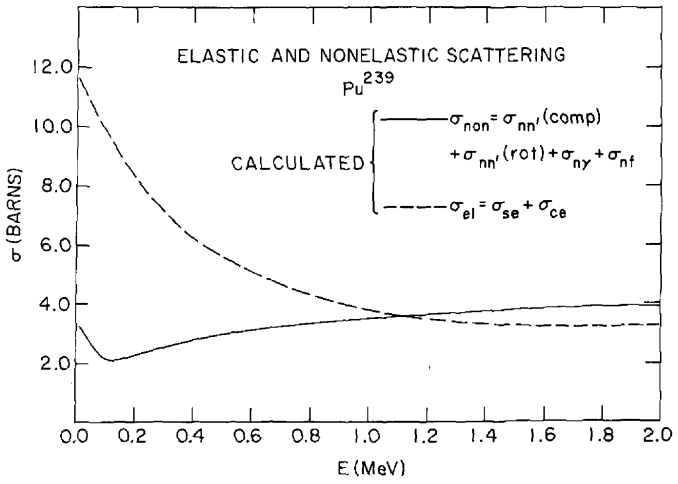

Figure 15

experimental constraints; namely, the total cross section σ_T, the potential scattering cross section σ_{pot}, and the s- and p-wave strength functions (S_0 and S_1).

Two additional pseudo-constraints σ_{nf} and $\sigma_{n\gamma}$ were also introduced in the statistical analysis such that the calculated values agreed to at least 5 to 7% of the most recent recommended values. The reason for the latter restriction is manifested in the fact that such an analysis would beget more confidence in the resulting inelastic processes.

These restrictions were very successful in providing a consistent set of parameters for performing calculations that produced very good agreement with all available experimental data from 10 keV to 20 MeV.

Theory

The differential cross sections for shape elastic scattering (σ_{SE}), the total reaction cross section (σ_R), and the direct inelastic scattering ($\sigma_{(rot)}$) were calculated using the Coupled Channel Code JUPITER I by Tamura[4].

In the phenomenological description it is assumed that the whole interaction to which the neutron is subjected may be described by an optical-model potenital $V(r,\theta,\varphi)$ which is complex and includes spin orbit coupling. Its radial dependence is of the Saxon-Woods form and its derivative. $V(r,\theta,\varphi)$ is assumed to be, in general, non-spherical and is defined as[4]:

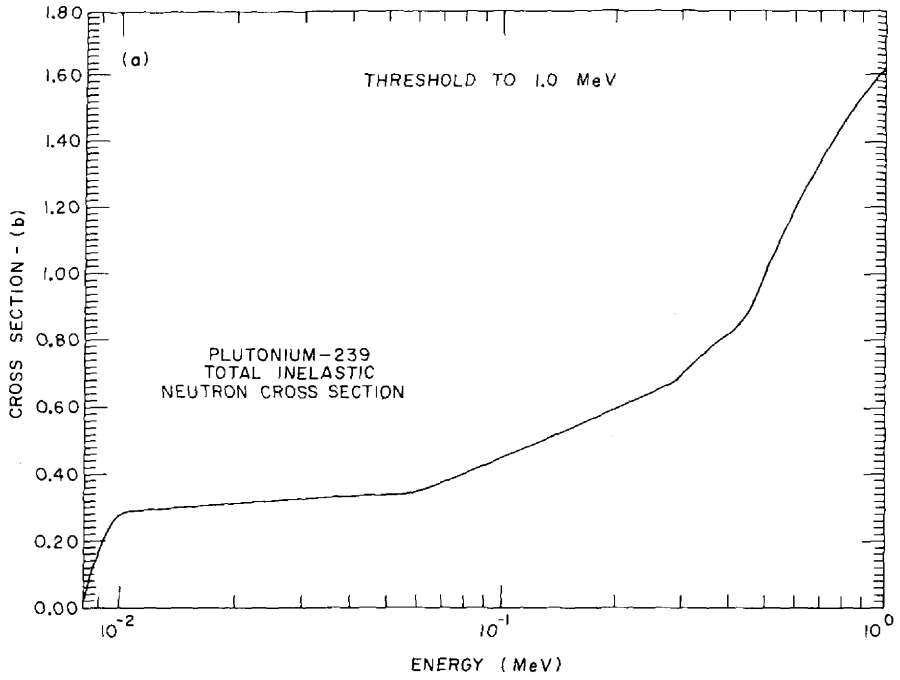

Figure 17

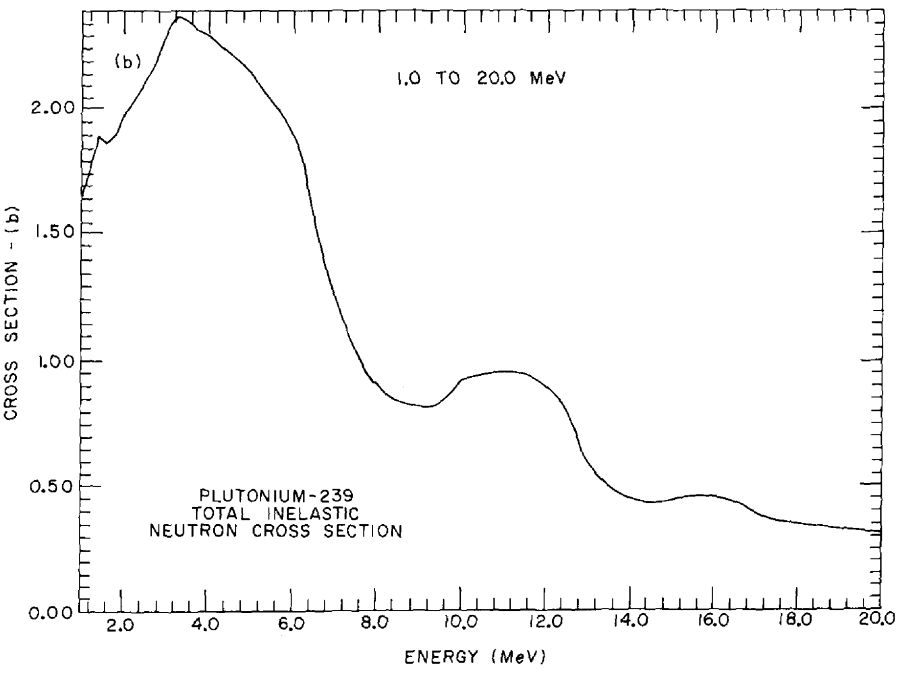

Figure 18

has steadily increased and in most cases exceeds the accuracy of experimental differential data. A clear example of the latter is the proper interpretation of the inelastic scattering cross sections for Pu-239.

An earlier evaluation of $\sigma_{nn'}$ and other reaction cross sections was presented at the Helsinki Conference, June 1970[1] (hereafter referred to as P). This analysis was to form the basis for the high energy (E > 100 keV) cross sections for the Evaluated Nuclear Data File (ENDF/B) on Pu-239. A subsequent meeting of the Cross Section Evaluation Working Group (CSEWG) resulted in expressions of concern that the elastic cross sections in ENDF/B-II were lower than those in ENDF/B-I and the inelastic cross sections were higher.

As pointed out in P, previous calculations used in evaluating Pu-239 have employed a spherical optical potential with the various reaction cross sections being interpreted as arising only from compound nucleus formation. However, since this nuclide is known to exhibit a high degree of deformity, the scattering of neutrons cannot be described adequately by the conventional optical model, which does not consider the coupling between the incident neutron motion and the nuclear surface rotation. This coupling causes the direct excitation of the rotational levels by inelastic scattering.

While these previous analyses have provided fairly good agreement between calculated and experimental angular distributions, the magnitude of the diffraction minima and maxima has not been well produced. Earlier investigations[2,3] have shown that neglecting the high degree of anistropy exhibited by the direct inelastic component can lead to serious errors in the prediction of the differential elastic and inelastic cross sections. These errors manifest themselves in two major areas. In the low

PLUTONIUM-239 INELASTIC CROSS SECTIONS

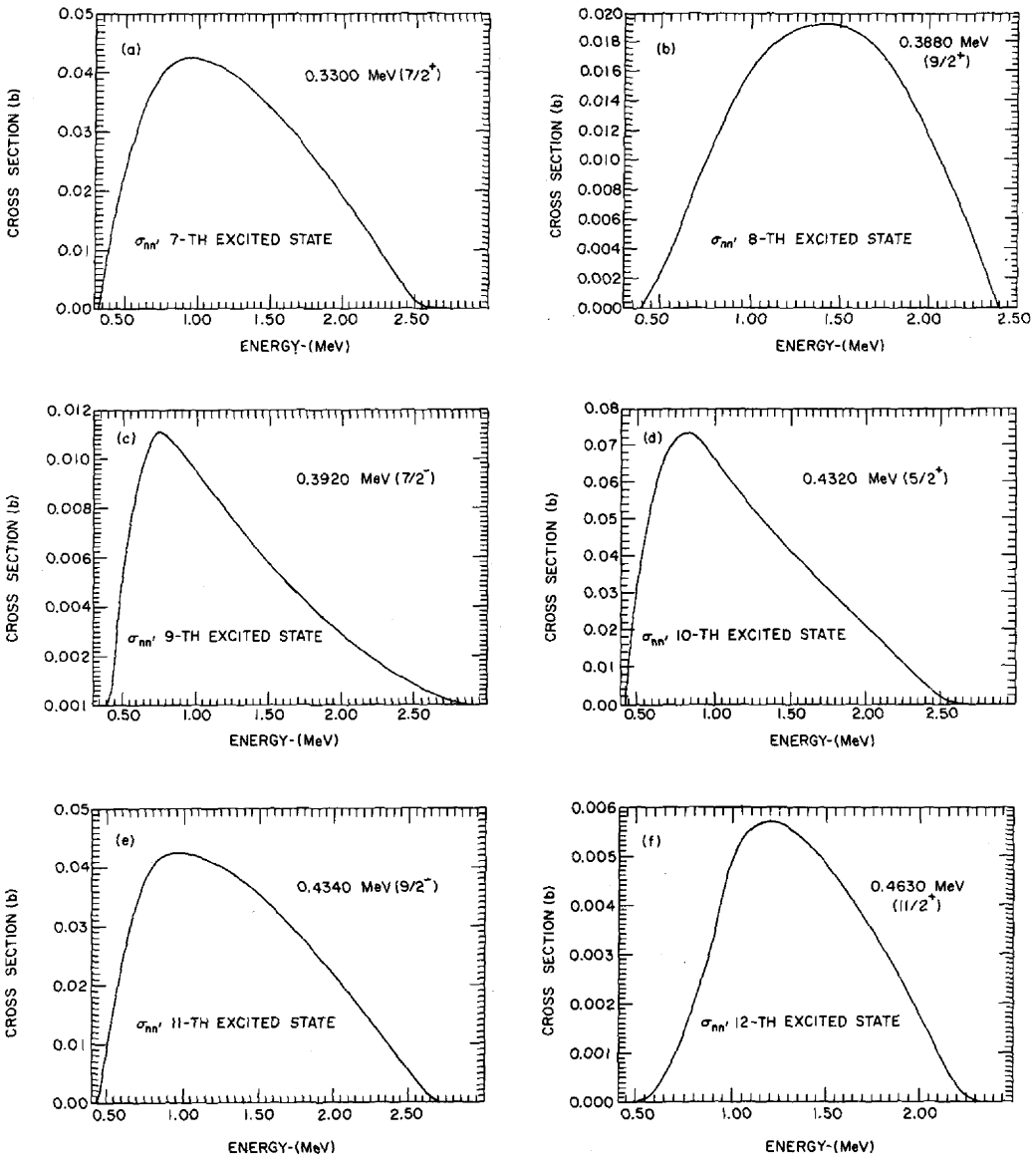

Figure 20

PLUTONIUM-239 INELASTIC CROSS SECTIONS

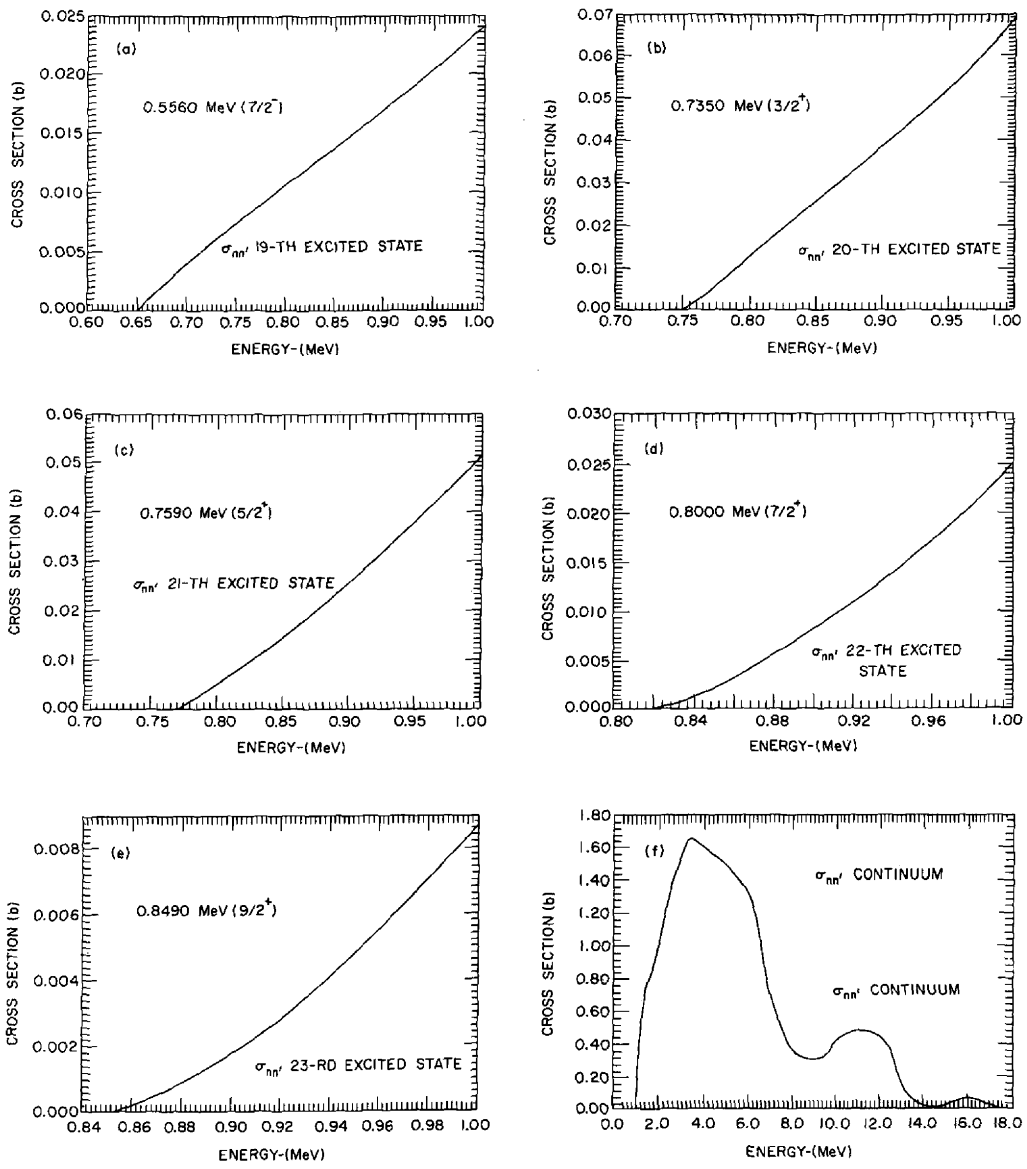

Figure 22

FIGURES

PLUTONIUM NEUTRON-PARTICLE CROSS SECTION

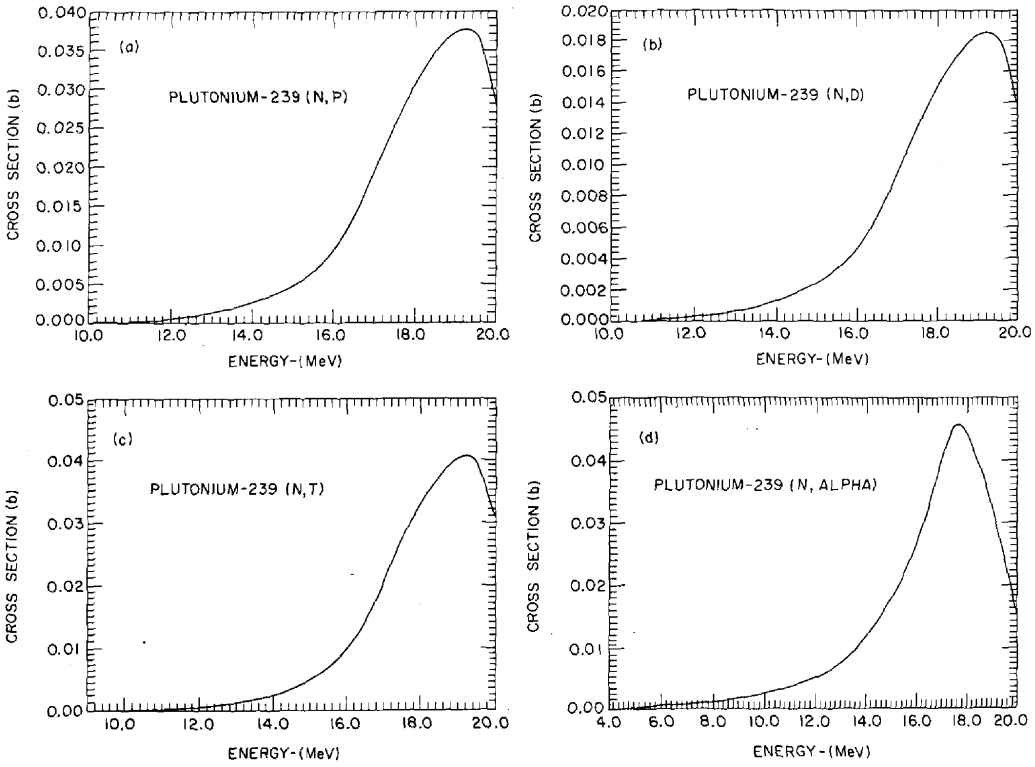

Figure 25

NOTICE

Printed in the United States of America
Available from
National Technical Information Service
U.S. Department of Commerce
5285 Port Royal Road
Springfield, Virginia 22151
Price: Printed Copy $3.00; Microfiche $0.95

June 1973 1100 copies